Chapter 5
Modeling the Laser Ablation Process

This chapter focuses on the problem of modeling the laser ablation process from a geometrical point of view. The objective is to create a model capable of describing the laser incision depth based on the knowledge of the laser parameters and inputs. The discussion starts with a statement of the problem, which is defined in terms of a supervised regression. Our approach is compared with existing heuristic models for the prediction of ablation depth.

Multiple parameters influence the laser ablation process. With regard to the surgical equipment in use today, these are laser power, delivery mode, pulse duration, scanning frequency. To fully understand the effects of these parameters, first we report on controlled experiments where only one parameter at a time is modified and the resulting depth of incision is examined.

The incision depth is modeled as a function of the laser exposure time. The inverse model is also extracted, which allows to calculate the exposure time required to reach a given incision depth. This inverse model is used in a feed forward setting, to prove the concept of the automatic incision of soft tissue. In addition, we demonstrate how the model can be used to implement the automatic ablation of entire volumes of tissue, through the superposition of controlled laser incisions. The chapter is concluded by a discussion of the findings for the depth estimation model, whose accuracy is considered from a clinical perspective.

5.1 Preliminary Considerations

The hypothesis formulated in Sect. 3.4 seeks to find a function f that relates the depth of the etch created by thermal laser ablation with the laser parameters. The geometry of the problem is illustrated in Fig. 5.1, which shows the creation of an incision by means of laser scans on a tissue target. The same simplifying assumptions used for temperature modeling are made here, i.e. that the slab of tissue presents a flat surface and that the laser is normally incident with respect to it. Without any loss of generality, here we restrict the motion of the laser to a straight line l, facilitating

L. Fichera, *Cognitive Supervision for Robot-Assisted Minimally Invasive Laser Surgery*, Springer Theses, DOI 10.1007/978-3-319-30330-7_5

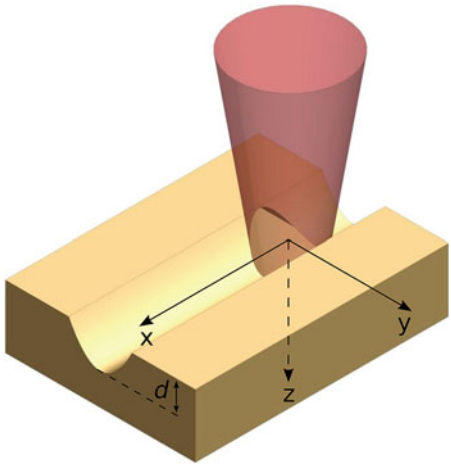

Fig. 5.1 Laser incision of soft tissue: rapid scans of the laser beam along an incision line l vaporize overlying layers of tissue with each pass. This process creates a crater on the surface of tissue, with depth d

the description of the methodology. The depth d of the incision depends on the combination of the following laser parameters: the laser power P, pulse duration τ, beam scanning frequency ω_s, plus the total laser exposure time t_{exp}. Because of the continuous nature of the output variable d, our problem is formulated in terms of a supervised regression problem: input/output data pairs are collected in order to understand and model the relation between the laser parameters and the resulting ablation depth.

Although the process we seek to model involves nonlinear physical phenomena, simple linear models exist in the literature, that provide predictions for the ablation depth based on the amount of laser energy delivered to the tissue [1].The analysis of these models provides useful directions to understand the nature of function f and, thus select an appropriate regression method for its approximation.

Prior research in the domain of laser-tissue interactions has established that the amount of material removed by thermal ablation depends primarily on the spatial distribution of energy density E [1, 2]. Estimations for the laser ablation depth can be computed by means of simple heuristic models. These are based on the assumption that material removal occurs as a continuous steady-state process, i.e. at a fixed, time-invariant rate. This assumption is legitimate if long laser pulses are used, i.e. $\tau > 1\mu s$ [1].

In a steady-state model, the removal of a unit mass of tissue requires the absorption of a fixed amount of energy, quantified by the *ablation enthalpy* h_{abl} ($J \cdot kg^{-1}$). Assuming a tissue with uniform density ρ, the relation between the depth of ablation d and the applied energy density E is described by [1]

$$d = \frac{E - E_{th}}{\rho \cdot h_{abl}}, \tag{5.1}$$

where E_{th} is the *ablation threshold*, i.e. the minimum amount of energy required to initiate the material removal process. Such threshold depends on the coefficient of absorption of tissue μ_a, according to the following relation

$$E_{th} = \frac{\rho \cdot h_{abl}}{\mu_a}. \tag{5.2}$$

Because of their simplicity, these models allow for a rapid, albeit rough estimation of the ablation depth. In practice, their application requires a prior determination of the ablation enthalpy h_{abl}, which is not straightforward to accomplish. Based on Eq. 5.1, this quantity can be estimated as the slope of a linear fitting between the ablation depth and the energy density,

$$h_{abl} = \frac{\Delta E}{\rho \Delta d}. \tag{5.3}$$

Nonetheless, this empirical method assumes that the energy density E emitted by the laser is entirely absorbed in the tissue: this assumption may not hold under all circumstances, since numerous factors exist that induce attenuations or alterations of the laser beam. For instance, previous studies have shown that absorption losses in the ablation plume can attenuate the laser energy up to 40 % of its theoretical value [1].

Despite the applicability issues mentioned above, steady-state models provide a basic understanding of the energetics of thermal ablation processes. These models postulate a linear relation between the ablation depth and the laser energy density E. This is surprising, especially in the light of our knowledge of the mechanisms involved in thermal ablation processes: the deposition of laser energy within tissue determines the onset of complex physical interactions, most of which are nonlinear in nature. Nonetheless, experimental studies show that under specific circumstances the relation between laser energy and ablation depth can be as simple as a linear function [3, 4], suggesting that the magnitude of nonlinear effects is neglectable.

5.2 Influencing Parameters

Our approach aims to extend the framework of steady-state models, investigating the individual contribution of each of the laser parameters. Understanding and modeling these contributions will allow for the creation of more explicit models of ablation depth, that use the same set of inputs used by clinicians during surgery, thus being straightforward to implement in a surgical context.

In this section we describe the experiments carried out to determine the influence of the energy delivery mode and the frequency of the laser scanning motion on the depth of incision produced by the laser exposure.

5.2.1 *Influence of Energy Delivery Mode*

Laser sources allow to control the rate of energy transfer by means of different *delivery modes*. In general, a delivery mode is defined by a function $m(t)$, which affects the energy density being delivered to the target according to the following equation:

$$E = \int_0^{t_{exp}} I\, m(t)\, dt. \tag{5.4}$$

An example is shown in Fig. 5.2, where the effects of two different delivery modes are contrasted: Continuous Wave (CW) and Repeated Pulse (RP). Using pulsed irradiation, the energy delivery process is slower, thus requiring additional exposure time to produce the same amount of energy density. When using the RP mode, the pulse duration (τ) needs to be configured. The laser source used in our experiments does not allow for an arbitrary value of duty cycle. Given a pulse duration, laser pulses are produced according to the following modulating function

$$m(t) = \sum_k (k)^{-1} H(t - k\tau), k \in \mathbb{N}, \tag{5.5}$$

where $H(t)$ is the Heaviside step function.

Here, the quantification of the effects of delivering the same amount of energy through different delivery modes was performed experimentally. To exclude the effects of laser motion on the resultant depth, single point incisions were performed, i.e. no scanning motion was applied to the laser beam, ($\omega_s = 0$). For these experiments, laser power was kept constant ($P = 2\,\text{W}$). We compared the effects of CW and RP ($\tau = 0.5\,\text{s}$) for increasing values of energy. The experiment involved three pairs

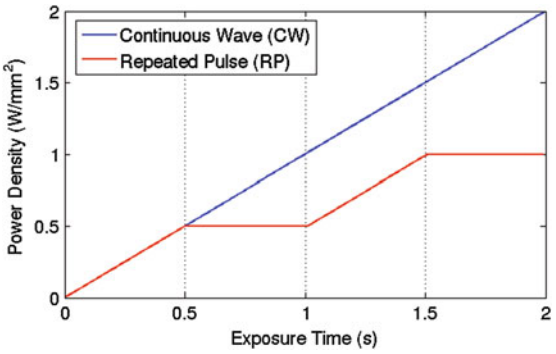

Fig. 5.2 Power densities transferred to tissue by a laser source ($I = 1\ \text{W} \cdot \text{mm}^{-2}$) by means of Continuous Wave (CW) and Repeated Pulse (RP) modes. For the RP mode, a pulse duration of 0.5 s and a duty-cycle of 50 % are considered. Reproduced from [5] with kind permission from John Wiley & Sons, Ltd

of experimental conditions. for each pair, we fixed the amount of energy involved. Experimental units were determined on the basis of actual values of energy used during real surgical interventions. Assigned values were 6, 10 and 15 joules. We performed ten repetitions for each configuration, resulting in a total of sixty ablations. Agar-based gel targets were used for this experiment.

Results

The examination of the produced ablation craters is illustrated in Fig. 5.3. Results are presented in Fig. 5.4. As expected, increasing energy densities resulted in deeper ablation craters. The experiment revealed that the ablation depth depends not just on the applied energy density, but also on the delivery mode. Under fixed energy conditions, the CW mode was found to produce, on average, deeper ablations. The difference between the mean ablation depths obtained in RP and CW was significant for values of energy equal to 10J ($p = 0.0125$) and 15J ($p = 0.0011$). In contrast, the difference was not significant at 6J ($p = 0.0823$).

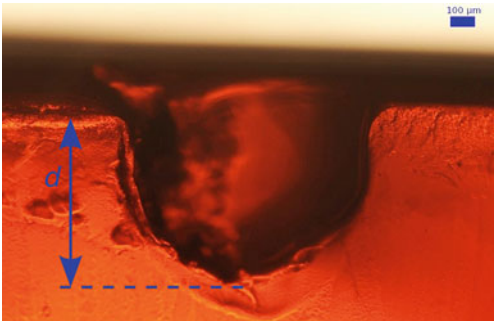

Fig. 5.3 Ablation crater produced on 2 % agar-based gel target. The resulting depth of incision d is indicated

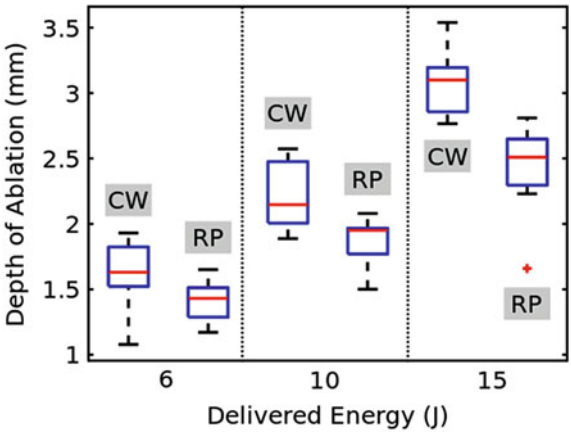

Fig. 5.4 Results of ablation depth produced with different energy delivery modes in agar-based gel targets. Reproduced from [5] with kind permission from John Wiley & Sons, Ltd

Table 5.1 Mean ($\bar{d}$), standard deviation (σ) and coefficient of variation (c_v) of ablation depths produced on agar-based gel targets through different delivery modes

Energy (J)	Delivery Mode	$\bar{d}$ (mm)	σ (mm)	c_v (%)
6	CW	1.619	0.266	16.4
	RP	1.410	0.162	11.4
10	CW	2.215	0.267	12.0
	RP	1.869	0.206	11.0
15	CW	3.075	0.254	8.2
	RP	2.421	0.356	14.7

Reproduced from [5] with kind permission from John Wiley & Sons, Ltd

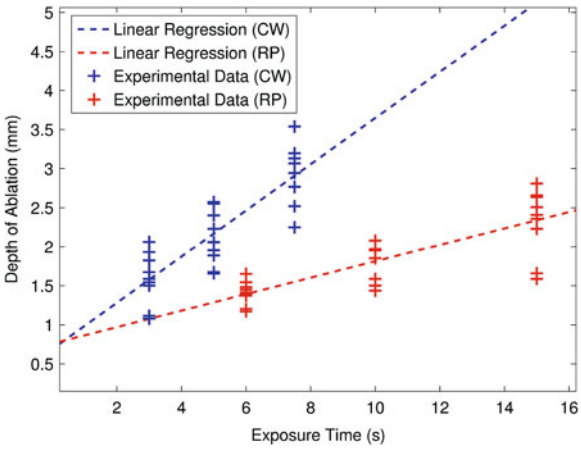

Fig. 5.5 Models of ablation depth in agar-based gel targets for Continuous Wave (*blue*) and Repeated Pulse mode (RP, *red*). Reproduced from [5] with kind permission from John Wiley & Sons, Ltd

Table 5.1 shows the average depth of incision for all the experiments; standard deviation and coefficient of variation are also listed. Observed variabilities have a marginal significance, as the coefficients of variation are all well below 20 %.

Further analysis of experimental data reveals that, once a delivery mode has been fixed, the ablation depth depends linearly on the applied exposure time. A simple linear regression is able to model the relation between these two quantities (Fig. 5.5) for both CW and RP. In both cases, the fitting error (normalized mean squared error, nMSE) is 0.02 %.

5.2.2 *Influence of Scanning Frequency*

Surgeons produce incisions by means of scans, i.e. movements of the laser beam along a trajectory on the surface of the tissue. The robotic platform used in this research [6, 7] offers automatic laser scanning, allowing for fast scans at a controlled frequency. Prior research has shown that there is a correlation between the speed of

motion of the laser and the resulting depth of incision in hard tissue [4]. We wish to determine if a similar relation holds true for soft tissue. Therefore, an experiment was performed to determine the influence of the laser scanning frequency on the depth of the resulting incision.

The laser beam was fired on the flat surface of agar-based gel targets, while it was automatically scanning along a line of fixed length ($l = 4.6$ mm). The scanning frequency was controlled through the scan time (t_s), which defined the time needed to move the beam back and forth along the pre-defined scan line. Three different values of scan time were considered: 30, 50 and 100 ms. We explored the effect of these speeds at increasing values of exposure time: 3–6 s with increments of 1 s. These values of scan time and exposure time are consistent with values typically used during surgery. For each combination of scan time/exposure time, nine repeated trials were executed, resulting in a total of 108 incisions. Constant laser power (3W) and delivery mode (CW) were used throughout the entire experiment.

Results

Results are shown in Fig. 5.6. Depending on the scan time, different depths of incision were obtained. The collected data shows that there is a correlation between scan time and the depth of the resulting incision cavity. Specifically, longer scan times are observed to produce deeper incisions.

Statistics of variability for these experiments are reported in Table 5.2. With respect to the energy delivery mode experiment, results are more uniform: observed standard deviations are one order of magnitude smaller, while the coefficients of variation are all below 13 %.

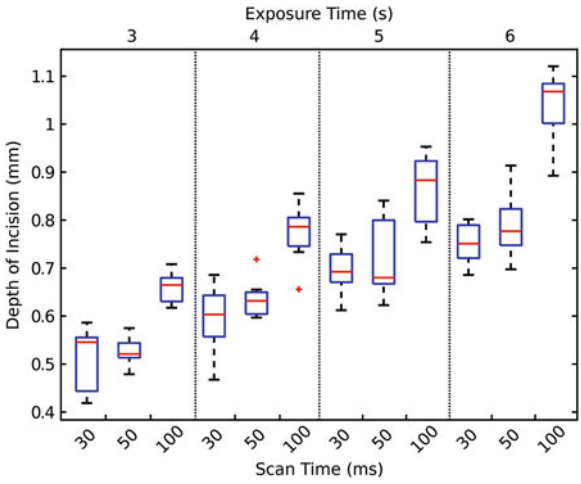

Fig. 5.6 Incision depths produced through different combinations of laser scan time/exposure time in agar-based gel targets. Reproduced from [5] with kind permission from John Wiley & Sons, Ltd

Table 5.2 Mean ($\bar{d}$), standard deviation (σ) and coefficient of variation (c_v) of ablation depths produced on agar-based gel targets through different values of scan time (t_s)

t_{exp} (s)	t_s (ms)	$\bar{d}$ (mm)	σ (mm)	c_v (%)
3	30	0.50	0.064	12.91
	50	0.63	0.037	5.9
	100	0.86	0.073	8.54
4	30	0.52	0.028	5.4
	50	0.77	0.056	7.32
	100	0.75	0.041	5.6
5	30	0.65	0.03	4.57
	50	0.69	0.045	6.69
	100	0.78	0.065	8.4
6	30	0.59	0.066	11.27
	50	0.72	0.081	11.27
	100	1.04	0.072	6.99

Reproduced from [5] with kind permission from John Wiley & Sons, Ltd

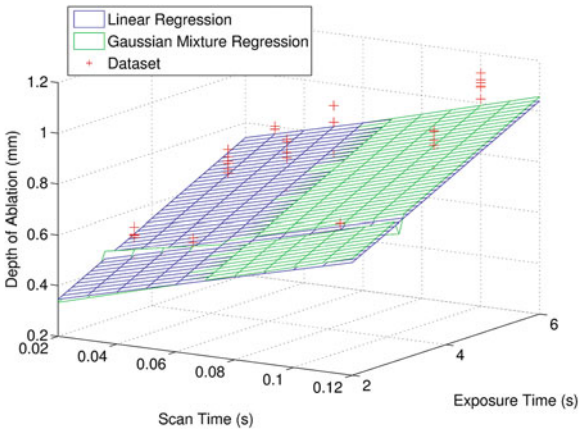

Fig. 5.7 Models of incision depth in agar-based gel targets for different combinations of scan time/exposure time. Reproduced from [5] with kind permission from John Wiley & Sons, Ltd

The combined influence of scan time and exposure time on the depth of incision is presented in Fig. 5.7. A simple linear regression of data fits the dataset with an error (normalized mean squared error, nMSE) of 0.6 %. A Gaussian mixture regression [8] was also evaluated, resulting in a fitting error of 0.8 %.

5.3 Incision Depth in Ex-Vivo Soft Tissue

During real interventions, surgeons set the laser parameters (power, delivery mode, scan time) before the execution of an incision. Exposure time is the only variable which is manipulated on-line in order to control the cutting process and the resulting

incision depth. In this section, we focus on the relation between incision depth and exposure time, with the aim of modeling it. Data used to produce this model was collected during experiments involving laser incision of ex-vivo soft tissue (chicken breast).

We propose that a function f exists, mapping the laser exposure time t_{exp} to the resulting depth of incision d,

$$d = f(t_{exp}) \tag{5.6}$$

Incisions were produced to obtain representative input/output data pairs $(\{t^i_{exp}, d^i\}_{i=1,\ldots,m})$ from which the function f could be estimated.

The input range for these experiments was selected in order to include values of exposure time typically used during real laser microsurgeries. The maximum exposure time in those cases is restricted by the fact that long exposures can produce thermal damage to the tissue [9, 10]. Surgeons aim to have an exposure time that is long enough for cutting, but still sufficiently short to avoid extensive damage to the surrounding tissue. Values of exposure time were chosen randomly in the selected range (0.5 5 s). A total of 54 incision trials were performed ($P = 3W$, Continuous Wave, $t_s = 0.1$ s, $l = 4.6$ mm).

Results

Typical incision craters observed during the examination of samples are shown in Fig. 5.8. The results are shown in Fig. 5.9. It can be seen that the relation between laser exposure time and incision depth is linear in this region of the input space. Collected data was randomized and divided into a training set and a validation set of 28 and 26 data points respectively. A simple least square minimization produced a linear estimation of the training set with Root Mean Square Error (RMSE) = 0.14 mm. The estimated rate of change of the depth was 0.28 mm/s for the specific laser parameters used. The accuracy of this model was evaluated on the validation set, where an error (RMSE) of 0.10 mm was obtained.

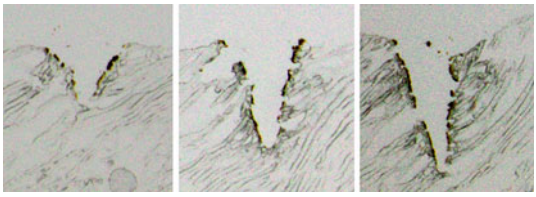

Fig. 5.8 Incision profiles produced with increasing exposure times (2.5, 3.5 and 4.5 s) and constant power density, scanning frequency and length. In order to get a complete exposure of the crater profile, targets were sectioned into thin slices (30 μm) with a cryostat microtome. Reproduced from [11]

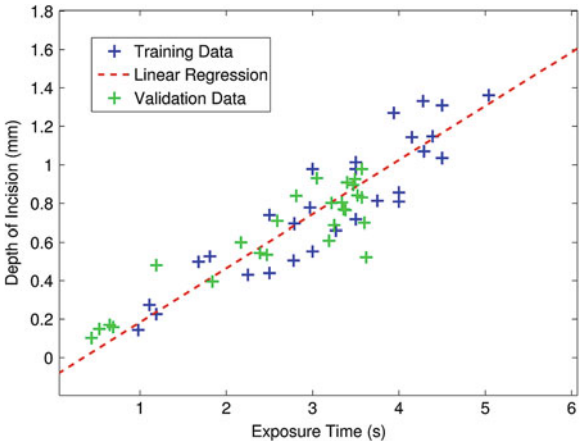

Fig. 5.9 Depth of incision in ex-vivo soft tissue for different exposure times. Reproduced from [5] with kind permission from John Wiley & Sons, Ltd

5.4 Inverse Model of Depth

Based on the linear model of depth derived in the previous section, here we create an inverse model, capable of estimating the exposure time ($\tilde{t}_{exp}$) required to achieve desired incision depths (a^*),

$$\tilde{t}_{exp} = f^{-1}(a^*). \tag{5.7}$$

This model is straightforward to obtain from the linear regression approximating Eq. 5.6. Implementing this model in the system, the exposure time is automatically controlled given a reference instead of an action.

In order to verify the quality of the estimations, five controlled experiments were conducted to estimate the prediction error. Table 5.3 shows the depths automatically obtained by the system when requiring a certain depth and using the inverse model. Discrepancies between the desired and the actual depths yield an error (RMSE) of 0.12 mm (Fig. 5.10).

Table 5.3 Results of the five automatic laser incision trials

a^* (mm)	$\tilde{t}_{exp}$ (s)	d (mm)
0.58	2.47	0.66
0.68	2.88	0.61
0.77	3.28	0.76
0.87	3.69	0.93
0.97	4.10	0.95

The desired depth $a*$ is mapped to the required exposure time $\tilde{t}_{exp}$ through an inverse model. The achieved depth d is reported in the rightmost column. Adapted from [12]

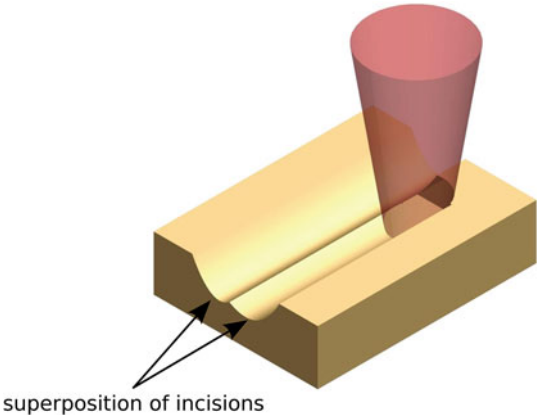

Fig. 5.10 Tissue ablation by incision superposition. Two (or more) incisions can be executed next to each other to ablate entire volumes of tissue

5.5 Ablation by Incision Superposition

Besides resecting tissue specimens and performing incisions, surgeons often require to completely eliminate blocks of tissue as part of surgical procedures. In the medical vocabulary this is known as *ablation*. This section presents a methodology to create controlled ablations based on the superposition of multiple incisions (see Fig. 5.10). The methodology uses the models of ablation depth derived in the previous section.

5.5.1 Ablation Model

Observing the linearity of the relationship between exposure time and incision depth, and assuming other thermal effects can be neglected (e.g., melting, carbonization) we hypothesize that the total effect of the laser exposure can be described as the sum of elemental exposures. In the case of using n incisions in parallel, the contour of the transverse plane $h(x)$ is then given by,

$$h(x) = \sum_{i}^{n} a_i \cdot \exp\left(\frac{-(x - b_i)^2}{2\sigma_i^2}\right) \tag{5.8}$$

where b_i represents the distance from the origin to the center of the ith incision. Fig. 5.11 shows an ablation generated adding four incisions. Using the model in (5.8) different strategies can be used to obtain the desired ablation depending on the required characteristics. One such strategy is described below.

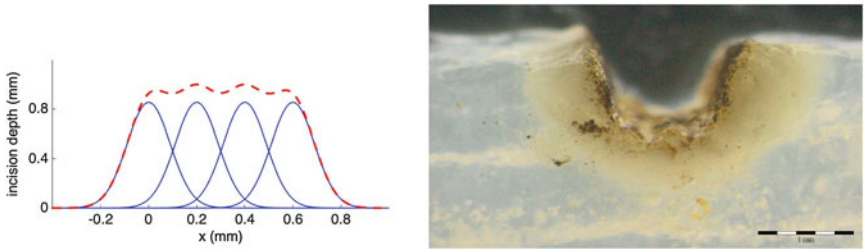

Fig. 5.11 Ablation by incision superposition. The graph on the *left* illustrates the concept: here, four incision profiles (*solid blue lines*) are combined to produce a larger ablation, whose profile is represented by the *dashed red line*. The figure on the *right* shows the transverse plane of an ablation cavity obtained by superimposing incisions on chicken muscle tissue. Adapted from [12]

5.5.2 Controlled Ablation

It can be shown that the sum of two identical Gaussians separated by a distance equal to the double of its standard deviation, i.e., $b_1 = 0, b_2 = 2\sigma$, results in a function whose maximum value is located in $(x = \sigma)$ and is given by,

$$h(\sigma) = \frac{2 \cdot a}{\sqrt{\exp(1)}} \tag{5.9}$$

Furthermore, it can be shown that the value of $h(x)$ is constant in an interval of the input space centered around $(x = \sigma)$, i.e. the function here presents a flat profile.[1]

These conditions can be used to perform a controlled ablation through the superposition of multiple incisions. A desired ablation depth (h^*) is mapped to the required incision amplitude using (5.9). The required exposure time can be obtained using the inverse model,

$$t_{exp} = f^{-1}\left(\frac{\sqrt{\exp(1)} \cdot h^*}{2}\right) \tag{5.10}$$

5.5.3 Ablation Assessment

In order to analyze the characteristics of the ablations, samples are examined under a microscope and differences among the profiles are analyzed. Repeatability of the ablation process can be studied defining a metric to compare among them. Ablation profiles are segmented, measuring the values for total width as well as depth in three different points of the crater (25, 50 and 75 % of the total width). Such metrics are described in Fig. 5.12.

[1] A proof is given in Appendix C.

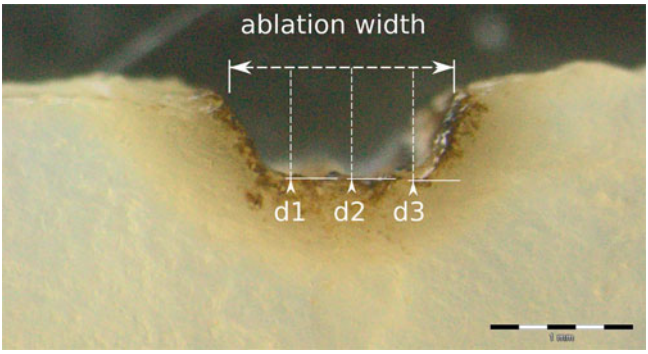

Fig. 5.12 Magnified view of an ablation profile created using the proposed automatic method. The depth of ablation is sampled in regular intervals along the ablation width. These measures are compared in order to evaluate the flatness of the ablation. Adapted from [12]

5.5.4 Results

Controlled Ablation

Four controlled ablations were created using the presented methodology. Given a desired ablation depth $h^* = 1.0$ mm, two incisions in parallel are required with a depth of $a^* = 0.824$ mm, which corresponds to an exposure time of $t_{exp} = 3.4$ s. Incisions must be separated a distance two times the estimated incision spread $b_2 = 2 \times \sigma$. An error (RMSE) of 0.17 mm was observed between the target depth h^* and the depths resulting from the ablations.

Ablation Assessment

The relative variability of the ablations was assessed comparing fourteen (14) ablation samples. Distribution of the observed ablation depths (d1, d2, d3) are graphically compared in Fig. 5.13. The mean ablation width was 1.62 mm.

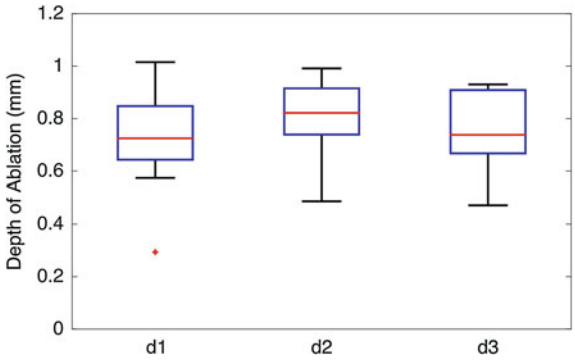

Fig. 5.13 Variability of the ablation depth at different points of the crater. The means are 0.72, 0.80 and 0.74 mm for d1, d2 and d3, respectively. Adapted from [12]

5.6 Discussion

The collected evidence shows that estimation of laser cutting depth in soft tissue can be enabled by a function that maps the laser exposure time to the resulting ablation depth. Such a function was extracted from experimental data. The described methodology allowed the creation of a model able to estimate the laser incision depth in ex-vivo chicken muscle tissue. A linear regression was found to adequately model the relation between exposure time and the laser incision depth. The model achieved a validation accuracy of 0.1 mm over incisions up to 1.4 mm deep produced on fresh ex-vivo tissue. The inverse model was used to control the laser incision depth, and to implement a strategy to perform controlled tissue ablation. The quality of the depth measurements was found to be a crucial aspect of the modeling methodology. Errors in the data can affect the function approximation task, producing inaccurate models. Although different from other methods found in the literature (e.g. confocal microscopy [13, 14]) Optical Coherence Tomography [15], Inline Coherent Imaging [16]), the protocol used in our research work presents a suitable resolution for the measurement of incision depths in the range of tenths of millimeters.

The proposed estimation method does not require any additional sensing device, thus it is appropriate for Transoral Laser Microsurgery (TLM). Considering the resection margins typically employed during TLM, we observe that the accuracy of the model is compatible with the requirements of these interventions. Surgeons aim to reach a minimum of 5 mm in resection depth to achieve surgical radicality [17, 18], i.e. to ensure the removal of the whole tumor. Smaller margins, down to 1 mm, are used in those cases where function preservation is considered, including the treatment of glottic cancer [17, 18]. However, it is important to point out that the reported accuracy was obtained on muscle tissue. Although it was used in the development of the proof-of-concept system, this type of tissue is not representative of the variety of tissues that are encountered during TLM, e.g. epithelium, muscle, adipose and fibrous tissues. These tissues present different optical properties [19], resulting in different laser absorption characteristics. This may mean that the ablation rate (mm/s) of these tissues differ from the linear relation that we have reported in this study for muscle tissue. The implementation of on-line estimation of incision depth in a real-case TLM scenario requires the availability of models able to account for the behavior of different types of tissues. Based on these observations, further experimental work might be required to study the ablation rate of different tissues and to find appropriate regression models.

All laser trials reported here present some degree of variability in the results, which can negatively affect the accuracy of the on-line depth estimation. This phenomenon has been observed in similar studies [4, 13, 14] and can be attributed to different factors. For example, instabilities of the laser source may affect the output power of the beam, producing deviations from intended values. Another limiting factor is represented by the inhomogeneous composition of biological tissue. These alterations influence the thermal interaction between laser radiation and tissue, thereby hindering the repeatability of laser incisions. However, the levels of variability observed in this

study were sufficiently small not to affect the reliability of the depth estimation. Errors observed during the ex-vivo incision trials support the conclusion that the model provides reliable estimations despite the mentioned repeatability issues.

References

1. A. Vogel, V. Venugopalan, Mechanisms of pulsed laser ablation of biological tissues. Chem. Rev. **103**(2), 577–644 (2003)
2. M. Niemz, *Laser-tissue Interactions* (Springer, Berlin, 2004)
3. K. Nahen, A. Vogel, Plume dynamics and shielding by the ablation plume during er:yag laser ablation. J. Biomed. Opt. **7**(2), 165–178 (2002)
4. S. Stopp, D. Svejdar, E. von Kienlin, H. Deppe, T.C. Lueth, A new approach for creating defined geometries by navigated laser ablation based on volumetric 3-d data. IEEE Trans. Biomed. Eng. 1872–1880 (2008)
5. L. Fichera, D. Pardo, P. Illiano, J. Ortiz, D.G. Caldwell, L.S. Mattos, Online estimation of laser incision depth for transoral microsurgery: approach and preliminary evaluation. Int. J. Med. Robot. Comput. Assist. Surg. (2015). http://dx.doi.org/10.1002/rcs.1656
6. L.S. Mattos, N. Deshpande, G. Barresi, L. Guastini, G. Peretti, A novel computerized surgeon machine interface for robot-assisted laser phonomicrosurgery. Laryngoscope **124**(8), 1887–1894 (2014)
7. L. Mattos, G. Dagnino, G. Becattini, M. Dellepiane, D. Caldwell, A virtual scalpel system for computer-assisted laser microsurgery. IEEE/RSJ Int. Conf. Intell. Robots Syst. (IROS) **2011**, 1359–1365 (2011)
8. S. Calinon, Robot Programming by Demonstration: A Probabilistic Approach (EPFL/CRC Press, 2009)
9. D. Pardo, L. Fichera, D. Caldwell, L. Mattos, Learning temperature dynamics on agar-based phantom tissue surface during single point co_2 laser exposure. Neural Process. Lett. **42**(1), 55–70 (2015). http://dx.doi.org/10.1007/s11063-014-9389-y
10. L. Fichera, D. Pardo, and L. S. Mattos, in *Supervisory System for Robot Assisted Laser Phonomicrosurgery*. Proceedings of the 35th International Conference of the IEEE Engineering in Medicine and Biology Society (EMBC), 2013
11. L. Fichera, D. Pardo, D.G. Caldwell, L.S. Mattos, in *New Assistive Technologies for Laser Microsurgery*. 4th Joint Workshop on New Technologies for Computer/Robot Assisted Surgery (CRAS-2014) (2014), pp. 60–63
12. L. Fichera, D. Pardo, P. Illiano, D. Caldwell, L. Mattos, in *Feed Forward Incision Control for Laser Microsurgery of Soft Tissue*. 2015 IEEE International Conference on Robotics and Automation (ICRA) (2015), pp. 1235–1240

13. L.A. Kahrs, J. Burgner, T. Klenzner, J. Raczkowsky, J. Schipper, H. Wörn, Planning and simulation of microsurgical laser bone ablation. Int. J. Comput. Assist. Radiol. Surg. **5**(2), 155–162 (2010)
14. J. Burgner, M. Müller, J. Raczkowsky, H. Wörn, Ex vivo accuracy evaluation for robot assisted laser bone ablation. Int. J. Med. Robot. Comput. Assist. Surg. **6**(4), 489–500 (2010)
15. H.W. Kang, J. Oh, A.J. Welch, Investigations on laser hard tissue ablation under various environments. Phys. Med. Biol. **53**(12), 3381 (2008)
16. B.Y. Leung, P.J. Webster, J.M. Fraser, V.X. Yang, Real-time guidance of thermal and ultrashort pulsed laser ablation in hard tissue using inline coherent imaging. Lasers Surg. Med. **44**(3), 249–256 (2012)
17. M.L. Hinni, A. Ferlito, M.S. Brandwein-Gensler, R.P. Takes, C.E. Silver, W.H. Westra, R.R. Seethala, J.P. Rodrigo, J. Corry, C.R. Bradford, J.L. Hunt, P. Strojan, K.O. Devaney, D.R. Gnepp, D.M. Hartl, L.P. Kowalski, A. Rinaldo, L. Barnes, Surgical margins in head and neck cancer: A contemporary review. Head Neck **35**(9), 1362–1370 (2013)
18. G. Mannelli, G. Meccariello, A. Deganello, V. Maio, D. Massi, O. Gallo, Impact of low-thermal-injury devices on margin ststus in laryngeal cancer. an experiment ex vivo study. Oral Oncol. **50**(1), 32–39 (2014)
19. S.L. Jacques, Optical properties of biological tissues: a review. Phys. Med. Biol. **58**(11), R37 (2013)